creative commons
COMMONS DEED

저작자표시-비영리-변경금지 2.0 대한민국

이용자는 아래의 조건을 따르는 경우에 한하여 자유롭게

- 이 저작물을 복제, 배포, 전송, 전시, 공연 및 방송할 수 있습니다.

다음과 같은 조건을 따라야 합니다:

저작자표시. 귀하는 원저작자를 표시하여야 합니다.

비영리. 귀하는 이 저작물을 영리 목적으로 이용할 수 없습니다.

변경금지. 귀하는 이 저작물을 개작, 변형 또는 가공할 수 없습니다.

- 귀하는, 이 저작물의 재이용이나 배포의 경우, 이 저작물에 적용된 이용허락조건을 명확하게 나타내어야 합니다.
- 저작권자로부터 별도의 허가를 받으면 이러한 조건들은 적용되지 않습니다.

저작권법에 따른 이용자의 권리는 위의 내용에 의하여 영향을 받지 않습니다.

이것은 이용허락규약(Legal Code)을 이해하기 쉽게 요약한 것입니다.

Disclaimer

dCollection

의학석사 학위논문

리툭시맙 치료를 받은 더블 익스프레서 미만성 큰 B 세포 림프종에서 스테리-스카이 패턴이 갖는 임상병리학적 및 분자유전학적 특징

Clinicopathologic and genetic features of starry-sky pattern in Rituximab-treated double expressor diffuse large B-cell lymphoma

울산대학교 대학원

의 학 과

성 현 정

리툭시맙 치료를 받은 더블 익스프레서 미만성 큰 B 세포 림프종에서 스테리-스카이 패턴이 갖는 임상병리학적 및 분자유전학적 특징

지도교수 고 현 정

이 논문을 의학석사 학위 논문으로 제출함

2023 년 08 월

울산대학교대학원

의 학 과

성 현 정

성현정의 의학석사학위 논문을 인준함

심사위원　　황 희 상 (인)

심사위원　　고 현 정 (인)

심사위원　　송 인 혜 (인)

울 산 대 학 교 대 학 원

2023 년　08 월

Abstract

Double expressor lymphoma (DEL) is a subset of diffuse large B-cell lymphoma (DLBCL) characterized by the co-expression of MYC and BCL2 proteins with a poor prognosis. However, there are no standard criteria for evaluating the morphologic features of DEL. We aimed to analyze the prognostic value of the starry-sky pattern (SSP) and its correlation with clinicopathologic and genetic features in 158 DEL cases. The SSP was significantly associated with aggressive parameters, including c-MYC overexpression, CD5 expression, higher International prognostic index (IPI), and higher age-adjusted IPI. In the univariate survival analyses, the presence of SSP was associated with unfavorable progression-free survival (PFS) ($p = 0.030$), and tended towards an adverse overall survival (OS) ($p = 0.065$). However, when c-MYC was overexpressed, SSP was significantly correlated with inferior OS ($p = 0.025$). In the multivariate survival analysis, SSP was also associated with poor PFS ($p = 0.049$). Additionally, next-generation sequencing data revealed DEL with SSP was significantly associated with the *KMT2D* mutation and had different genetic mutation profiles from DEL without SSP. In conclusion, SSP may represent morphologic characteristics of aggressiveness in DEL.

Keywords: Double expressor lymphoma, Starry-sky pattern, Diffuse large B-cell lymphoma, c-MYC, Prognosis, *KMT2D*

Table of Contents

Abstract ····· i

Table of contents ····· ii

List of tables and figures ····· iii

Introduction ····· 1

Materials and Methods ····· 3

1. Patient selection and clinical parameters ····· 3
2. Morphologic analyses ····· 3
3. Immunophenotypic evaluation ····· 5
4. Fluorescence in situ hybridization (FISH) analyses ····· 5
5. Targeted next-generation sequencing (NGS) ····· 6
6. Statistical analysis ····· 6

Results ····· 8

1. Baseline characteristics of all patients ····· 8
2. Morphologic analyses ····· 8
3. Clinicopathological and immunophenotypic analyses ····· 10
4. Fluorescence in situ hybridization (FISH) analyses ····· 12
5. Targeted next-generation sequencing (NGS) analyses ····· 12
6. Survival analysis of morphologic features in double expressor lymphoma ····· 13

Discussion ····· 17

Conclusion ····· 20

References ····· 21

Supplementary appendix ····· 25

국문요약 ····· 31

List of tables and figures

Table 1. Baseline characteristics of the enrolled patients ····· 9

Table 2. Comparison of clinicopathologic parameters between the SSP and non-SSP groups ····· 11

Table 3. Univariate and multivariate Cox proportional hazard analysis for overall survival and progression-free survival ····· 16

Figure 1. Representative images for SSP and DEL ····· 4

Figure 2. Targeted NGS analysis of 22 DEL cases ····· 13

Figure 3. Kaplan–Meier survival curves for overall survival (OS) and progression-free survival (PFS) according to the presence of starry-sky pattern (SSP) ····· 14

Introduction

Diffuse large B-cell lymphoma (DLBCL) exhibits a broad spectrum of clinicopathological and genetic features that reflect its underlying biological heterogeneity.[1-3] Based on gene expression profiling, DLBCL can be stratified into two distinct cell-of-origin (COO) subtypes: germinal center B-cell-like (GCB) and activated B-cell-like (ABC).

Patients with high-risk DLBCL subtypes may have poor outcomes, including higher rates of relapsed or refractory disease following front-line immunochemotherapy R-CHOP (rituximab plus cyclophosphamide, doxorubicin, vincristine, and prednisone).[4,5] Double expressor lymphoma (DEL) is a high-risk subtype of DLBCL characterized by the overexpression of the c-MYC and BCL2 proteins without underlying gene rearrangement. Although DEL is not a distinct biological entity in the 5th edition of the WHO Classification of Tumours of Haematopoietic and Lymphoid Tissues and the International Consensus Classification (ICC) of Mature Lymphoid Neoplasms, it accounts for approximately 30% of DLBCL cases and is associated with an aggressive clinical course and an increased risk of central nervous system (CNS) relapse.[6,7]

Genomic research on DLBCL has identified diverse molecular mechanisms underlying the disease and has contributed to the identification of important genetic alterations with therapeutic and prognostic implications.[8] Several gene alterations, including *TP53*, *MYD88*, *CDKN2A*, or *BCL2*, are significantly associated with worse prognosis in DLBCL.[4,9-11] Recent studies have revealed that DEL can occur in GCB and ABC subtypes, arising from heterogeneous molecular and genomic backgrounds, but it is more frequently observed in the ABC subtype.[1,8] However, the clinicopathological and molecular features of DEL remain poorly characterized due to limited research.

The "starry-sky" pattern (SSP) is a characteristic feature almost exclusively observed in hematolymphoid neoplasms, particularly in Burkitt lymphoma; however, it has also been observed in other lymphoma subtypes, including DLBCL. Although uncommon, the SSP is evident in 5–10% of DLBCL cases.[12] The "*starry*" component is characterized by scattered tingible body macrophages with abundant pale cytoplasm mixed with a background of monomorphic lymphoma cells.[13] The tingible bodies are intracellular remnants of degenerated

cells resulting from phagocytosis of dead and dying neoplastic cells. Therefore, the presence of SSP indicates high rates of mitosis and apoptosis.[14]

The underlying mechanism of SSP in hematolymphoid malignancies remains elusive, and research in the area is lacking. However, a correlation between SSP and MYC rearrangement has been observed.[12] Bouroumeau et al. identified an association between the SSP in DLBCL and c-MYC overexpression, correlating with better survival in c-MYC-positive-DLBCL.[14] Despite the potential importance of SSP in lymphoma, very few studies have investigated its histopathological characteristics in DEL. Therefore, our study aimed to elucidate the relationship between SSP and various clinicopathologic and molecular features of DEL.

Materials and methods

Patient selection and clinical parameters

We retrospectively reviewed 654 patients primarily diagnosed with DLBCL by excisional biopsy, surgical resection, or needle biopsy treated at Asan Medical Center between January 2013 and December 2021. All patients underwent rituximab-based chemotherapy for first-line treatment. Among them, we identified 158 patients (24.1%) diagnosed with DEL. We defined MYC or BCL2 expression as positive when more than 40% or 50% of cells, respectively, showed expression, per previous reports.[1] Corresponding medical records were reviewed to obtain clinical information. Overall survival (OS) was defined as the date of death or the date of final follow-up from the day of initial diagnosis. Progression-free survival (PFS) was defined as the day of progression, recurrence, patient death, or final follow-up from the day of initial diagnosis.

Morphological analysis

Morphological analysis was performed on entire slides using hematoxylin and eosin staining. We evaluated the proportion of tumor cell areas showing a "starry-sky" appearance while defining the presence of SSP as more than 10% of the tumor cell area. A representative image of SSP is presented in Figure 1A. Additionally, we assessed the presence of tumor necrosis and cytological subtypes according to the WHO classification, which included centroblastic, immunoblastic, and anaplastic.

Figure 1. Representative image for SSP and DEL. (A) Tingible body macrophages in the background of tumor cells are notable features of SSP (hematoxylin & eosin [H&E], ×200); (B) Strong nuclear staining for c-MYC is indicative of c-MYC overexpression in the SSP group. (immunohistochemistry [IHC], ×200); (C) Membranous staining for CD5 in the SSP group (IHC, ×200); (D) Ki-67 for the SSP group (IHC, ×200) (E) H&E images for the non-SSP group; (F) Weak expression for c-MYC in the non-SSP group (IHC, ×200); (G) Negative staining for CD5 in the non-SSP group (IHC, ×200); (H) Ki-67 for the non-SSP group (IHC, ×200).

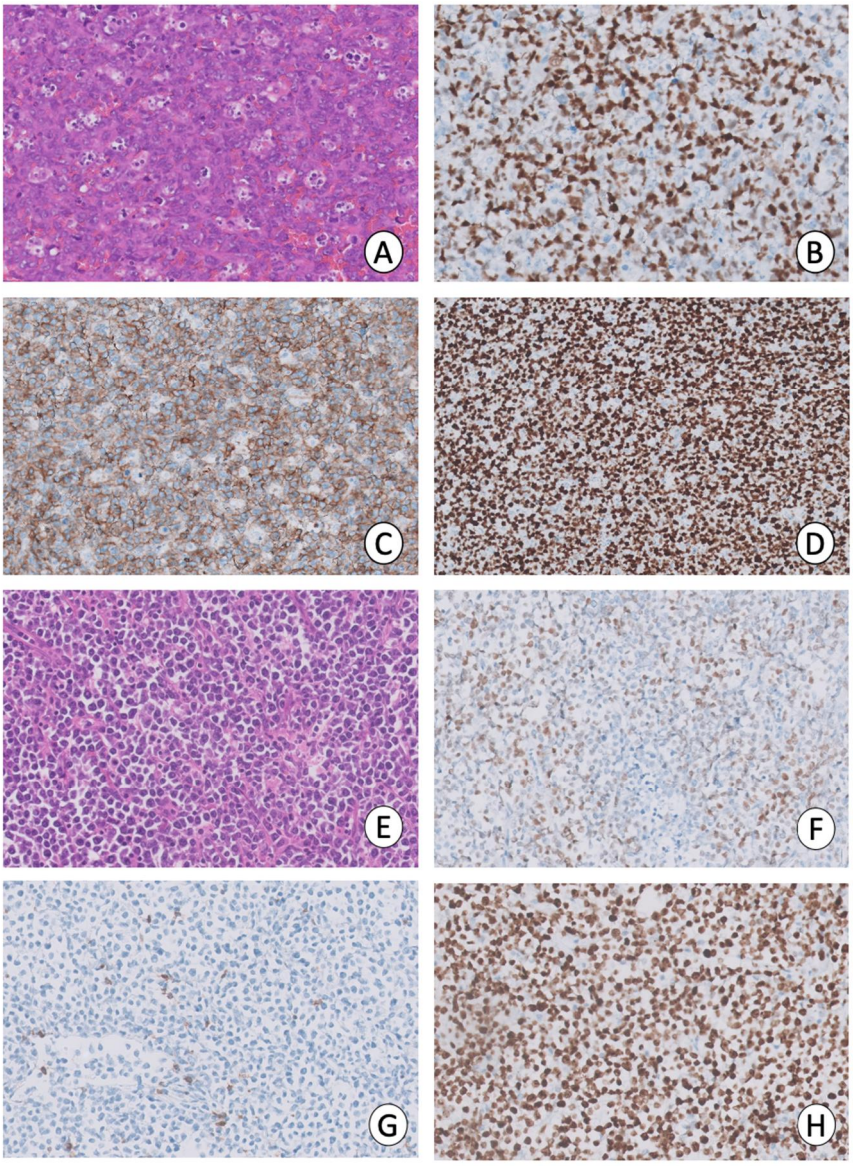

Immunophenotypic evaluation

Immunohistochemistry (IHC) was performed on 4 μm thick sections cut from whole slide levels using a OptiView DAB IHC Detection Kit on the BenchMark XT automatic immunostaining device (Ventana Medical Systems, Tucson, AZ, USA) according to the manufacturer's instructions. Seven antibodies were used for each slide: c-MYC, BCL2, BCL6, CD10, CD5, MUM-1, and Ki-67 (See Supplementary Appendix, Table S1). Detection of EBV was performed on paraffin sections using the BenchMark XT automatic immunostaining device (Ventana Medical Systems, Tucson, AZ, USA) according to the manufacturer's instructions. Sections were visualized by Ventana EBER ISH iView Blue Detection Kit (Catalog no.800-092, Ventana) and INFORM EBER probe (Catalog no.800-2842, Ventana). For c-MYC and BCL-2, the immunoreactive score (IRS) described by Remmele and Stenger was calculated.[15,16] The IRS was determined by multiplying the percentage of positive cells by staining intensity, which was interpreted as a 4-tier score, ranging from 0 (no expression) to 3+ (strong expression). We classified high IRS as more than the median value of each IRS. BCL-6 expression was considered high when 30% or more of the tumor cells were immunoreactive for BCL-6. The Ki-67 labeling index was determined by dividing the number of positive nuclei by the total number of counted nuclei (%) under high magnification (400×) in the highest labeling area, which was estimated by eyeballing. The cut-off value for a high Ki-67 labeling index was set at 85% based on the studies of Yoon et al.[17] IHC staining was scored blindly by two pathologists (H.J.S. and H.G.), and discordant cases were subjected to joint proofreading. Antibodies against BCL6, CD10, and MUM-1 were used to classify subtypes based on the Hans algorithm.[18]

Fluorescence in situ hybridization (FISH) analysis

We retrospectively reviewed the results of FISH studies and targeted next-generation sequencing (NGS) results performed for diagnostic purposes. In total, 114, 71, and 67 FISH cases were reviewed for *MYC*, *BCL2*, and *BCL6* genes, respectively. FISH was performed using the Vysis LSI dual-color break-apart rearrangement probes (Abbott, Abbott Park, IL, USA) per the manufacturer's protocol. Sixty tumor cells were evaluated for translocation and copy number gain of the corresponding genes using the process used for routine diagnosis.

The cut-off value for showing rearrangement was at least 10% of the tumor cells exhibiting split signals and copy number gain (CNG) was adopted from a recent study, indicating that CNGs are tumor cells with three or more copies.[19]

Targeted NGS

For DNA extraction, we used 6-μm-thick slices from each formalin-fixed paraffin-embedded (FFPE) tissue section. We performed targeted NGS on 22 cases using the Illumina MiSeq platform (Illumina, San Diego, CA, USA) with OncoPanel Lymphoma version 1.2, which which was developed and validated by our institution and interrogates the complete exonic sequence of 258 genes and introns of seven genes involved in rearrangement based on previous literature on DLBCL.[2,3,8,10,20] The specific genes are listed in Supplementary Table 2. Two hundred nanograms of genomic DNA was fragmented by sonication (Covaris Inc., Woburn, MA, US) to an average size of 250 bp, followed by size selection using Agencourt AMPure XP beads (Beckman Coulter, Brea, CA, USA). A DNA library was prepared by sequential reactions of end repair, A-tailing, and ligation with a TruSeq adaptor, using a SureSelectXT Reagent kit (Agilent Technologies, Santa Clara, CA)). Each library was addressed with sample-specific barcodes of 6 bp and quantified using Qubit dsDNA HS Assay Kit (ThermoFisher Scientific, Waltham, MA, USA). Eight libraries were pooled to a total of 750 ng for hybrid capture using an Agilent SureSelectXT custom kit (OP_AMCv3 RNA bait; Agilent Technologies).

Statistical analysis

All data analyses were conducted using the SPSS Statistics software (Version 24.0; IBM Corp., Armonk, NY, USA) and R version 4.0.5 (R Foundation for Statistical Computing, Vienna, Austria). The chi-squared and Fisher's exact tests were used to compare categorical variables. The Student's *t*-test and Mann–Whitney *U* test were used for comparison of continuous variables. The Kaplan–Meier method was used to calculate OS and PFS, and the log-rank test was employed to compare survival between groups. Univariate and multivariable regression analyses were performed using the Cox proportional hazard model. Statistical significance was considered when p-values were lower than 0.05.

Ethical statement

This study was approved by the Institutional Review Board of Asan Medical Center (Approval No., 20220252). The requirement for informed patient consent was waived upon the de-identification process. All procedures followed the ethical standards of the responsible committee on human experimentation (institutional and national) and were in line with the Helsinki Declaration of 1975, revised in 2008.

Results

Baseline characteristics of all patients

The baseline characteristics of the 158 patients enrolled in this study are summarized in Table 1. The median age of the patients was 67 years (range, 24–93), and sex was evenly distributed, with a slight predominance of female patients (52.5%). One hundred and fifty-three cases (96.8%) were classified as DLBCL-NOS, and one was classified as primary diffuse large B cell lymphoma of the CNS. The remaining four cases were DLBCL arising from follicular lymphoma or post-transplant lymphoproliferative disease. All patients received rituximab-based chemotherapy as frontline treatment. Based on the Hans algorithm, approximately three-fourths of the cases were classified as the ABC subtype, reflecting a higher frequency of this subtype in DEL.

Morphologic analyses

The SSP was observed in one-fourth of the DEL cases (42/158, 26.5%). The distribution of SSP in DEL was heterogeneous, ranging from 10% to 90% of the tumor area. All cases showed diffuse effacement of architecture by tumor cells. Coagulative necrosis was observed in 41 cases (26%). Most cases (89.9%) exhibited centroblastic features, followed by immunoblastic (7.6%), and anaplastic (2.5%) features, according to morphologic variants.

Table 1. Baseline characteristics of the enrolled patients

Patient characteristics	Total (N = 158)	SSP group (n = 42)	Non-SSP group (n = 116)	*P*-value
Age at diagnosis (years)	64.3 ± 14.0	64.9 ± 12.7	64.1 ± 14.5	0.284
Sex				1.000
Male	75 (47.5%)	20 (47.6%)	55 (47.4%)	
Female	83 (52.5%)	22 (52.4%)	61 (52.6%)	
DLBCL subtype (Hans algorithm)				0.838
GCB	41 (25.9%)	10 (23.8%)	31 (26.7%)	
Non-GCB	117 (74.1%)	32 (76.2%)	85 (73.3%)	
Extranodal involvement	82 (51.9%)	24 (57.1%)	58 (50.0%)	0.474
Bone marrow involvement	33 (20.9%)	10 (23.8%)	23 (19.8%)	0.263
Serum LDH elevation	91 (57.6%)	27 (64.3%)	64 (55.2%)	0.364
Presence of B-symptoms	28 (17.7%)	6 (14.3%)	22 (19.0%)	0.639
Ann Arbor staging classification				0.213
I	21 (13.3%)	3 (7.1%)	18 (15.5%)	
II	30 (19.0%)	6 (14.3%)	24 (20.7%)	
III	14 (8.9%)	6 (14.3%)	8 (6.9%)	
IV	93 (58.9%)	27 (64.3%)	66 (56.9%)	
IPI risk group				0.285
Low	20 (12.6%)	2 (4.8%)	18 (15.5%)	
Low-int.	15 (9.5%)	2 (4.8%)	13 (11.2%)	
High-int.	90 (57.0%)	27 (64.3%)	63 (54.3%)	
High	33 (20.9%)	11 (26.1%)	22 (19.0%)	
Number of relapsed patients	33 (20.9%)	11 (26.2%)	22 (19.0%)	0.377
CNS relapse	12 (7.6%)	2 (4.8%)	10 (8.6%)	0.518
Follow-up period (months)	30.0 ± 24.6	22.3 ± 19.0	32.8 ± 25.8	0.039
Double-hit lymphoma	9 (5.6%)	3 (7.1%)	6 (5.1%)	
Triple-hit lymphoma	1 (0.6%)	1 (2.3%)	0 (0%)	

Values are represented as number (%) or mean ± standard deviation (SD), unless otherwise indicated.

GCB: germinal center B-cell like; ABC: activated B-cell like; IPI: International Prognostic Index; CNS: central nervous system.

Clinicopathological and immunophenotypic parameters associated with SSP

The main clinicopathologic parameters according to the presence of SSP are summarized in Table 2. The SSP was significantly correlated with high IRS for c-MYC ($p = 0.027$) in DEL (Figure 1B). In addition, c-MYC expression in tumor cells was significantly higher in SSP group than Non-SSP group. ($p < 0.001$, Mann-Whitney test; Supplemantary Fig. 1A). We, additionally, further divided into two groups with a ≥ 70% cutoff for c-MYC high expression, according to the previous reports[21,22] : 45 cases c-MYC high expression (≥ 70%) and 113 c-MYC intermediate expression (≥ 40% and <70%). The SSP extent (the ratios of the proportion of tumor cell areas showing the SSP) is significantly increased in the c-MYC high expression group. ($p = 0.036$, Mann-Whitney tests; Supplemantary Fig. 1B)

CD5 expression of tumor cells in DLBCL is an aggressive prognostic factor.[1] We observed CD5 positivity in 23 cases (14.6%), the expression of which was associated with the SSP in DEL ($p = 0.046$) (Figure 1C). Interestingly, 113 (71.5%) cases showed a high Ki-67 labeling index; however, Ki-67 labeling index did not show statistically significant difference between SSP group and non-SSP group ($p = 0.842$) (Figures 1D&H). Only two cases presented a positive EBER ISH result in a few small lymphocytes. Additionally, the presence of the SSP in DEL showed a significant association with higher IPI and age-adjusted IPI ($p = 0.029$ and 0.030, respectively).

Table 2. Comparison of clinicopathologic parameters between the SSP and non-SSP groups

Clinicopathologic parameters	SSP group (n = 42)	Non-SSP group (n = 116)	*P*-value
BCL2 (IRS)			0.720
High	20 (47.6%)	60 (51.7%)	
Low	22 (52.4%)	56 (48.3%)	
c-MYC (IRS)			**0.027**
High	25 (59.5%)	46 (39.7%)	
Low	17 (40.5%)	70 (60.3%)	
BCL6 (IHC)			0.747
Positive (≥30%)	38 (90.5%)	107 (92.2%)	
Negative (<30%)	4 (9.5%)	9 (7.8%)	
CD5 (IHC)			**0.046**
Positive	10 (23.8%)	18 (11.2%)	
Negative	32 (76.2%)	24 (88.8%)	
Ki67 labeling index (%)			0.842
High (≥85%)	31 (73.8%)	82 (70.7%)	
Low (<85%)	11 (26.2%)	34 (29.3%)	
IPI			**0.029**
High (3–5)	38 (90.5%)	85 (73.3%)	
Low (0–2)	4 (9.5%)	31 (26.7%)	
Age-adjusted IPI			**0.030**
High (2–3)	30 (71.4%)	60 (51.7%)	
Low (0–1)	12 (28.6%)	56 (48.3%)	

Values are represented as number (%). IRS: immunoreactive score; IHC: immunohistochemistry.

FISH analyses

Nine cases of double-hit lymphoma and one case of triple-hit lymphoma were identified through FISH analysis. Among these cases, four (44%) showed starry-sky morphology. Among a total of 114 cases in which *MYC* FISH was performed, *MYC* translocation was observed in 23.3% (7/30) of SSP cases and 22.6% (19/84) of non-SSP cases. Copy number gain of the *MYC* gene was observed in three cases (10%) with SSP and 11 cases (13.1%) without SSP. However, no statistically significant correlation was found between SSP and gene rearrangement or copy number status in *MYC*. Although we analyzed gene rearrangement or copy number status in *BCL2* and *BCL6*, we did not observe any association with SSP. (See Supplementary Material, Table S3).

Targeted NGS analyses according to SSP

The NGS sequencing results for 22 DEL cases were analyzed and correlated with SSP morphology (Figure 2). The most frequent mutated gene was *CDKN2A* (8/22, 36.3%), followed by *CDKN2B, PIM1*, and *TP53,* which were in line with mutational profiles of the non-SSP group. In contrast, *KMT2D* (6/8, 75.0%) and *MYD88* (3/8, 37.5%) mutations were the most frequently mutated genes in the SSP group. SSP DEL was significantly associated with *KMT2D* mutations, as six out of eight cases showed *KMT2D* mutations compared with only one out of 14 DEL cases without SSP (odds ratio [OR] = 38.96, $p = 0.006$). Among them, three were nonsense mutations, and two were frameshift mutations. The remaining showed the splice-site mutations. However, the presence of SSP was not significantly correlated with any specific mutational profile except for *KMT2D*. Interestingly, *CCND3, TCF3*, and *ID3* gene mutations, which are frequently mutated in sporadic Burkitt lymphoma, were not found in all 9 SSP DELs, but infrequently found in non-SSP DELs (8%, 1/13, each).

Figure 2. Targeted NGS analysis of 22 DEL cases.

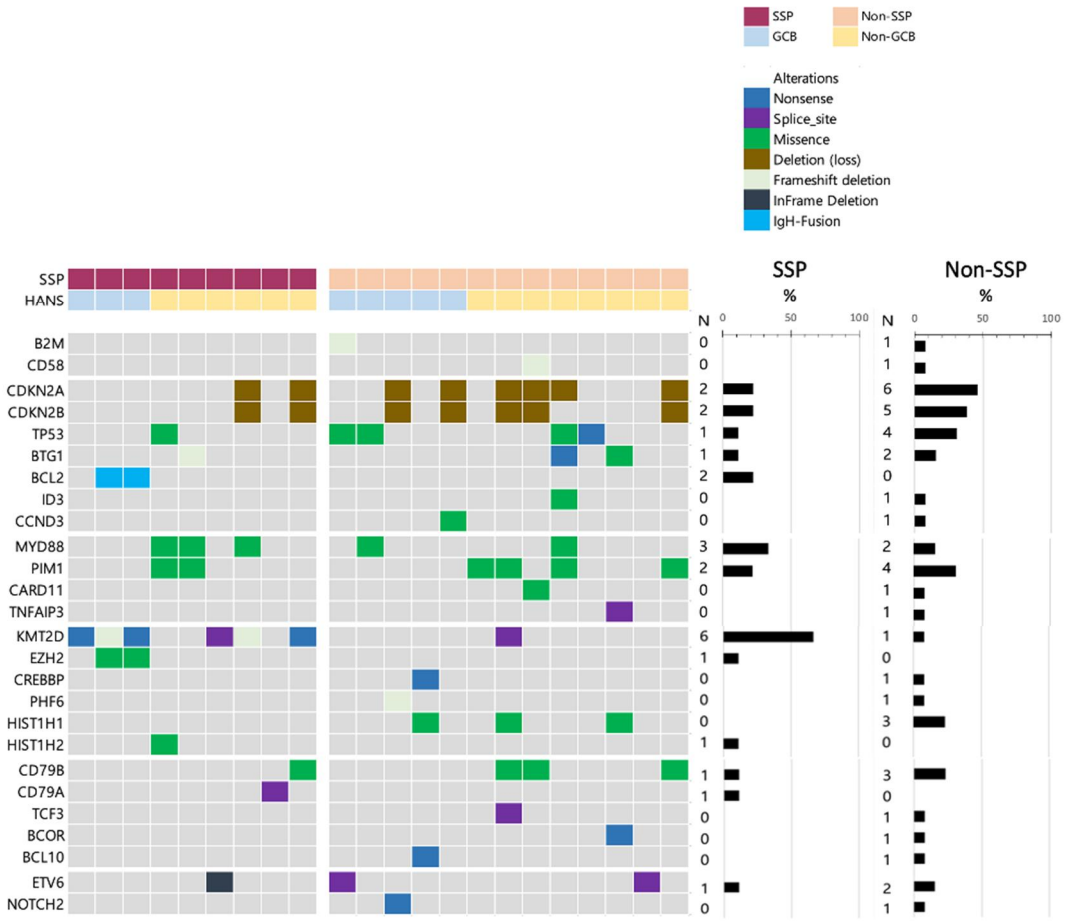

Survival analysis of morphologic features in double expressor lymphoma

The results of the univariate survival analyses according to the status of SSP in the rituximab-treated patients of DEL are presented in Figures 3A–B. The patients with SSP had significantly lower PFS than those without (p = 0.030). However, there was no statistically significant difference in OS between the two groups, although the presence of SSP tended to have a marginal statistical significance (p = 0.064).

Figure 3. (A-B) Kaplan–Meier survival curves for (A) OS and (B) PFS show a significantly shorter PFS for the SSP group than that for the non-SSP group. The OS of the SSP group was also inferior compared to that of the non-SSP group; (C-D) Survival curves for c-MYC overexpression status; (C) OS for the SSP group is significantly worse than that of the non-SSP group. (D) PFS was not significantly different.

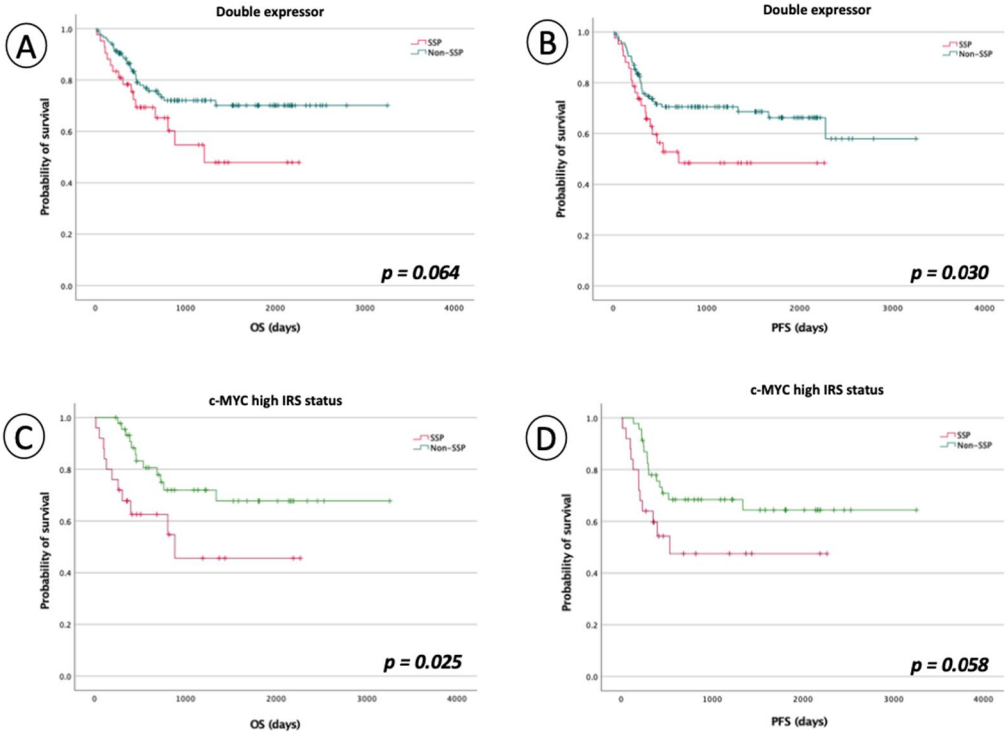

Additionally, in the c-MYC high group, the presence of SSP had a significant association with lower OS (p = 0.025) and marginal significance on poor PFS (p = 0.058) (Figure 3C-D). We also evaluated the impact of other morphologic features, such as cell type and tumor necrosis on OS and PFS, but found no significant correlation (Supplementary Figure 1A-D). Our findings indicate that SSP could have a unique morphologic feature, stratifying survival outcomes in patients in DEL.

In addition, the prognostic difference between OS and PFS was not significant in the ABC subgroup (Supplementary Figures 3A–B). In the univariate Cox proportional hazard analyses, SSP was identified as a unique histologic feature showing a superior prognostic impact on OS and PFS (Table 3). Multivariate survival analyses were conducted to confirm the prognostic relevance of the presence of SSP (Table 3). Patients in the SSP group displayed significantly poorer PFS in the adjustment of age-adjusted IPI risk group, old age, and B-symptom status (hazard ratio [HR]: 1.801, 95% confidence interval [CI]: 1.003–3.235, $p = 0.049$). The SSP group also exhibited a tendency for poor OS (HR: 1.759, 95% CI: 0.934–3.315, $p = 0.081$). Only the high-risk group of the age-adjusted IPI classifier and B-symptom status was associated with significantly poor OS and PFS, which could be attributed to the relatively small number of enrolled cases.

Table 3. Univariate and multivariate Cox proportional hazard analysis for overall survival and progression-free survival

Parameter	Univariate analysis		Multivariate analysis	
	Hazard ratio (95% CI)	*P*-value	Hazard ratio (95% CI)	*P*-value
PFS				
Presence of starry-sky pattern	1.764 (1.0004–3.101)	0.049	1.801 (1.003–3.235)	0.049
Age > 60 years	1.437 (0.800–2.582)	0.225	1.482 (0.820–2.681)	0.193
Age-adjusted IPI 2-3 (vs. 0–1)	3.060 (1.633–5.734)	<0.001	2.410 (1.253–4.633)	0.008
B-symptom	2.688 (1.493–4.840)	<0.001	2.276 (1.224–4.233)	0.009
Necrosis	1.311 (0.731–2.353)	0.364	-	
Cell type: Centroblastic	1		-	
Immunoblastic	1.046 (0.377–2.903)	0.931	-	
Anaplastic	0.750 (0.103–5.435)	0.776	-	
OS				
Presence of starry-sky pattern	1.779 (0.964–3.281)	0.065	1.759 (0.934–3.315)	0.081
Age > 60 years	1.593 (0.834–3.040)	0.158	1.635 (0.851–3.138)	0.140
Age-adjusted IPI 2–3 (vs. 0-1)	4.492 (2.087–9.672)	<0.001	3.499 (1.581–7.745)	0.002
B-symptom	3.005 (1.591–5.676)	<0.001	2.313 (1.189–4.498)	0.014
Necrosis	1.380 (0.734–2.595)	0.318	-	
Cell type: Centroblastic	1		-	
Immunoblastic	1.210 (0.433–3.381)	0.716	-	
Anaplastic	-	-	-	

Discussion

Our study aimed to evaluate the clinicopathologic and genetic characteristics and prognostic significance of the morphologic features, particularly the SSP, in R-CHOP-treated DEL. In this study, SSP was identified in 26.5% of cases–more than double the cases in DLBCL.[13,24] DEL showed higher IPI, age-adjusted IPI, and ABC-subtype predominance, in line with previous reports. [4,5,25-30] Although the SSP indicates a high turnover rate in lymphoma, our study did not identify a correlation with a high Ki-67 labeling index. The mean Ki-67 labeling index in our DEL cohort was 86.4% (standard deviation 10.6%), significantly higher than the average value in DLBCL. Interestingly, the SSP and non-SSP groups showed a high Ki-67 labeling index in over 70% of cases, suggesting that the high proliferation rate of DEL may have reduced the difference between the groups.

While Oliveira et al. demonstrated a correlation between *MYC* gene translocation and SSP in the DLBCL group, we did not find such an association in our DEL group study.[31] However, we did observe a significant correlation between c-MYC overexpression and SSP in DEL (p = 0.027). Previous literature has shown similar results in that c-MYC overexpression in DLBCL was significantly associated with the presence of SSP.[14]

Previous studies have identified CD5 expression as an independent prognostic factor in DLBCL, which is correlated with concurrent expression of BCL2 and c-MYC.[32,33] Our study found that CD5 positivity in DEL is associated with SSP. This finding is consistent with previous reports that CD5 expression is associated with aggressive clinical behavior and poor prognosis in DLBCL.

We found no correlation between SSP and gene rearrangement or copy number status in the FISH studies. Therefore, we suggest that starry-sky appearance is possibly related to the activation of MYC and BCL2 proteins outside of gene rearrangement. In sporadic Burkitt lymphoma , *ID3-TCF3-CCND3* pathway genes were frequently mutated, which are involved in cell survival and proliferation, and these mutations are thought to contribute to the development of characteristic SSP.[34] In contrast, genetic alterations of DEL reflect cumulative mutations involving B-cell receptors and NFκB pathways, such as *MYD88, CD79B,* and *PIM*,[5,6,22] which were also identified in our studies. We also found a significantly higher

frequency of *KMT2D* mutation in DEL with SSP. Given that *KMT2D* mutations may promote overgrowth by distrubing the expression of tumor suppressor genes that control B-cell activating pathways, SSP in DEL may represent tangible body macrophage-mediated tumor growth.[35] Tumorigenesis may be enhanced by the maintenance of an anti-inflammatory microenvironment during tumor progression and the production of IL-10 by tissue-based macrophages may increase B-cell survival factors. However, we could not find a correlation with other genetic mutations, especially related to apoptosis and the cell cycle in Burkitt lymphoma, although we found a relatively high Ki-67 proliferation index in our DEL cases. We suggest that the proliferation-related mechanism in DEL is different from Burkitt lymphoma, and therefore, the mechanism underlying the SSP may also differ between the two entities. In addition, we also observed the possibility that SSP in DEL may have a different genetic mutation profile than non-SSP. Further studies with larger sample sizes are needed to confirm the association between starry-sky appearance and specific genetic mutations in DEL.

Xu-Monette et al. discovered that MYC/BCL2 double-expression had a significant adverse prognostic impact only within the EZB genetic subtype and LymphGen-unclassified subtype according to LymphGen classification.[22] Additionally, they observed that *KMT2D* mutation had adverse prognostic significance in DEL cases but not non-DEL cases, and the most frequent *KMT2D* mutations were associated with EZB subtype.[22,36] Given that the EZB genetic subtype is enriched in the GCB subtype based on the gene-expression subgroup and the ABC subtype is more frequent in DEL, we indicated the prognostic significance of *KMT2D* mutation in DEL would be associated with the presence of SSP rather than the Hans classification.[36]

Bouroumeau et al. showed that c-MYC-positive DLBCL with SSP had better OS than those without SSP and suggested a negative effect of c-MYC overexpression on survival could be lost by SSP, indicating that high levels of apoptosis could be a protective factor in c-MYC-positive DLBCL.[14] However, when compounded by BCL2 co-expression, our study revealed SSP has an adverse effect on survival; additionally, SSP was associated with inferior prognosis in cases with c-MYC overexpression in DEL. Although the biological mechanisms of DEL remain unclear, SSP in DEL represents malignant outgrowth accelerated by c-MYC expression. A complementary multivariate analysis on a larger cohort could strengthen the link between

these variables.

Our study has several limitations. First, there would be potential interpretation bias in assessing the presence and extent of SSP. To minimize the representativeness issues caused by selection bias, we reviewed the entire slides from the collected cases. Second, the sample size of cases with NGS data was relatively small, which may not fully reflect the genetic heterogeneity of DEL. We could not evaluate the prognostic impact of *KMT2D* mutation in our cohort due to the limited number of cases. Additionally, our study was retrospective in nature, and selection bias may have influenced our results. Therefore, larger prospective studies are needed to confirm our findings and investigate the clinical significance of SSP.

Conclusion

We suggest SSP in DEL may associated with *KMT2D* mutations in different molecular backgrounds from Burkitt lymphoma. Given that the presence of SSP has been associated with aggressive clinicopathologic and genetic markers, starry-sky appearance may represent morphological characteristics of aggressiveness in DEL and may be a useful marker for identifying inferior prognosis. We suggest that identifying SSP may have important implications for pathologists when evaluating histologic samples.

References

1. Sehn LH, Salles G. Diffuse Large B-Cell Lymphoma. *N Engl J Med.* 2021;384(9):842-858.

2. Mendeville M, Janssen J, Kim Y, van Dijk E, de Jong D, Ylstra B. A bioinformatics perspective on molecular classification of diffuse large B-cell lymphoma. *Leukemia.* 2022;36(9):2177-2179.

3. Lenz G, Wright G, Dave SS, et al. Stromal Gene Signatures in Large-B-Cell Lymphomas. *New England Journal of Medicine.* 2008;359(22):2313-2323.

4. Landsburg DJ, Hughes ME, Koike A, et al. Outcomes of patients with relapsed/refractory double-expressor B-cell lymphoma treated with ibrutinib monotherapy. *Blood Adv.* 2019;3(2):132-135.

5. Hu S, Xu-Monette ZY, Tzankov A, et al. MYC/BCL2 protein coexpression contributes to the inferior survival of activated B-cell subtype of diffuse large B-cell lymphoma and demonstrates high-risk gene expression signatures: a report from The International DLBCL Rituximab-CHOP Consortium Program. *Blood.* 2013;121(20):4021-4031; quiz 4250.

6. Alaggio R, Amador C, Anagnostopoulos I, et al. The 5th edition of the World Health Organization Classification of Haematolymphoid Tumours: Lymphoid Neoplasms. *Leukemia.* 2022;36(7):1720-1748.

7. Campo E, Jaffe ES, Cook JR, et al. The International Consensus Classification of Mature Lymphoid Neoplasms: a report from the Clinical Advisory Committee. *Blood.* 2022;140(11):1229-1253.

8. Chen H, Qin Y, Liu P, et al. Genetic Profiling of Diffuse Large B-Cell Lymphoma: A Comparison Between Double-Expressor Lymphoma and Non-Double-Expressor Lymphoma. *Molecular Diagnosis & Therapy.* 2022.

9. Jardin F, Jais JP, Molina TJ, et al. Diffuse large B-cell lymphomas with CDKN2A deletion have a distinct gene expression signature and a poor prognosis under R-CHOP treatment: a GELA study. *Blood.* 2010;116(7):1092-1104.

10. Xu-Monette ZY, Wu L, Visco C, et al. Mutational profile and prognostic significance

of TP53 in diffuse large B-cell lymphoma patients treated with R-CHOP: report from an International DLBCL Rituximab-CHOP Consortium Program Study. *Blood.* 2012;120(19):3986-3996.

11. Dubois S, Viailly PJ, Bohers E, et al. Biological and Clinical Relevance of Associated Genomic Alterations in MYD88 L265P and non-L265P-Mutated Diffuse Large B-Cell Lymphoma: Analysis of 361 Cases. *Clin Cancer Res.* 2017;23(9):2232-2244.

12. Dy-Ledesma JL, Khoury JD, Agbay RLMC, Garcia M, Miranda RN, Medeiros LJ. Starry Sky Pattern in Hematopoietic Neoplasms: A Review of Pathophysiology and Differential Diagnosis. *Advances in Anatomic Pathology.* 2016;23(6):343-355.

13. Dy-Ledesma JL, Khoury JD, Agbay RL, Garcia M, Miranda RN, Medeiros LJ. Starry Sky Pattern in Hematopoietic Neoplasms: A Review of Pathophysiology and Differential Diagnosis. *Adv Anat Pathol.* 2016;23(6):343-355.

14. Bouroumeau A, Bussot L, Bonnefoix T, et al. c-MYC and p53 expression highlight starry-sky pattern as a favourable prognostic feature in R-CHOP-treated diffuse large B-cell lymphoma. *J Pathol Clin Res.* 2021;7(6):604-615.

15. Remmele W, Stegner HE. [Recommendation for uniform definition of an immunoreactive score (IRS) for immunohistochemical estrogen receptor detection (ER-ICA) in breast cancer tissue]. *Pathologe.* 1987;8(3):138-140.

16. Fedchenko N, Reifenrath J. Different approaches for interpretation and reporting of immunohistochemistry analysis results in the bone tissue - a review. *Diagn Pathol.* 2014;9:221.

17. Yoon DH, Choi DR, Ahn HJ, et al. Ki-67 expression as a prognostic factor in diffuse large B-cell lymphoma patients treated with rituximab plus CHOP. *European Journal of Haematology.* 2010;85(2):149-157.

18. Hans CP, Weisenburger DD, Greiner TC, et al. Confirmation of the molecular classification of diffuse large B-cell lymphoma by immunohistochemistry using a tissue microarray. *Blood.* 2004;103(1):275-282.

19. Quesada AE, Medeiros LJ, Desai PA, et al. Increased MYC copy number is an independent prognostic factor in patients with diffuse large B-cell lymphoma. *Mod Pathol.* 2017;30(12):1688-1697.

20. Lenz G, Wright GW, Emre NCT, et al. Molecular subtypes of diffuse large B-cell

lymphoma arise by distinct genetic pathways. *Proceedings of the National Academy of Sciences*. 2008;105(36):13520-13525.

21. Xu-Monette ZY, Dabaja BS, Wang X, et al. Clinical features, tumor biology, and prognosis associated with MYC rearrangement and Myc overexpression in diffuse large B-cell lymphoma patients treated with rituximab-CHOP. *Mod Pathol*. 2015;28(12):1555-1573.

22. Xu-Monette ZY, Wei L, Fang X, et al. Genetic Subtyping and Phenotypic Characterization of the Immune Microenvironment and MYC/BCL2 Double Expression Reveal Heterogeneity in Diffuse Large B-cell Lymphoma. *Clin Cancer Res*. 2022;28(5):972-983.

23. Schmitz R, Young RM, Ceribelli M, et al. Burkitt lymphoma pathogenesis and therapeutic targets from structural and functional genomics. *Nature*. 2012;490(7418):116-120.

24. Chuang S-S, Ye H, Du M-Q, et al. Histopathology and Immunohistochemistry in Distinguishing Burkitt Lymphoma From Diffuse Large B-Cell Lymphoma With Very High Proliferation Index and With or Without a Starry-Sky Pattern: A Comparative Study With EBER and FISH. *American Journal of Clinical Pathology*. 2007;128(4):558-564.

25. Johnson NA, Slack GW, Savage KJ, et al. Concurrent expression of MYC and BCL2 in diffuse large B-cell lymphoma treated with rituximab plus cyclophosphamide, doxorubicin, vincristine, and prednisone. *J Clin Oncol*. 2012;30(28):3452-3459.

26. Hashmi AA, Iftikhar SN, Nargus G, et al. Double-Expressor Phenotype (BCL-2/c-MYC Co-expression) of Diffuse Large B-Cell Lymphoma and Its Clinicopathological Correlation. *Cureus*. 2021;13(2):e13155.

27. Rosenthal A, Younes A. High grade B-cell lymphoma with rearrangements of MYC and BCL2 and/or BCL6: Double hit and triple hit lymphomas and double expressing lymphoma. *Blood Rev*. 2017;31(2):37-42.

28. Savage KJ, Slack GW, Mottok A, et al. Impact of dual expression of MYC and BCL2 by immunohistochemistry on the risk of CNS relapse in DLBCL. *Blood*. 2016;127(18):2182-2188.

29. Hwang J, Suh C, Kim K, et al. The Incidence and Treatment Response of Double Expression of MYC and BCL2 in Patients with Diffuse Large B-Cell Lymphoma: A Systematic Review and Meta-Analysis. *Cancers (Basel)*. 2021;13(13).

30. Aggarwal A, Rafei H, Alakeel F, et al. Outcome of Patients with Double-Expressor Lymphomas (DELs) Treated with R-CHOP or R-EPOCH. *Blood.* 2016;128(22):5396-5396.

31. Oliveira CC, Maciel-Guerra H, Kucko L, et al. Double-hit lymphomas: clinical, morphological, immunohistochemical and cytogenetic study in a series of Brazilian patients with high-grade non-Hodgkin lymphoma. *Diagn Pathol.* 2017;12(1):3.

32. Na HY, Choe JY, Shin SA, et al. Characteristics of CD5-positive diffuse large B-cell lymphoma among Koreans: High incidence of BCL2 and MYC double-expressors. *PLoS One.* 2019;14(10):e0224247.

33. Durani U, Ansell SM. CD5+ diffuse large B-cell lymphoma: a narrative review. *Leukemia & Lymphoma.* 2021;62(13):3078-3086.

34. Campo E. New pathogenic mechanisms in Burkitt lymphoma. *Nature Genetics.* 2012;44(12):1288-1289.

35. Ortega-Molina A, Boss IW, Canela A, et al. The histone lysine methyltransferase KMT2D sustains a gene expression program that represses B cell lymphoma development. *Nature Medicine.* 2015;21(10):1199-1208.

36. Wright GW, Huang DW, Phelan JD, et al. A Probabilistic Classification Tool for Genetic Subtypes of Diffuse Large B Cell Lymphoma with Therapeutic Implications. *Cancer Cell.* 2020;37(4):551-568.e514.

Supplementary Appendix

Table S1. Antibodies used for immunohistochemistry

Antibody (clone)	Type	Dilution	Retrieval solution	Source
BCL2 (124)	Mouse monoclonal	1:25	Ventana CC1 (Ventana Medical Systems Inc., Tucson, AZ, USA)	Dako (Glostrup, Denmark)
c-MYC (EP121)	Rabbit monoclonal	1:50	Ventana CC1 (Ventana Medical Systems Inc.)	Cell Marque (Rocklin, CA, USA)
BCL6 (GI191E/A8)	Mouse monoclonal	1:50	Ventana CC1 (Ventana Medical Systems Inc.)	Cell Marque
CD10 (56C6)	Mouse monoclonal	1:100	Ventana CC1 (Ventana Medical Systems Inc.)	Novocastra (Newcastle, UK)
CD5 (4C7)	Mouse monoclonal	1:100	Ventana CC1 (Ventana Medical Systems Inc.)	Novocastra
MUM-1 (MUM1P)	Mouse monoclonal	1:100	Ventana CC1 (Ventana Medical Systems Inc.)	Dako
Ki-67 (MIB1)	Mouse monoclonal	1:200	Ventana CC1 (Ventana Medical Systems Inc.)	Dako
Cyclin D1 (SP4)	Mouse monoclonal	1:100	Ventana CC1 (Ventana Medical Systems Inc.)	Cell Marque

Table S2. Specific gene list for targeted next-generation sequencing

DNA Gene List: Entire Exonic Sequence for the Detection of Base Substitution, Insertions/Deletions, and Copy Number Alterations

ABL1, ABL2, ACTB, AKT 1, ALK, ANKRD11, ANKRD26, APC, ARID1A, ASXL1, ATM, ATR, AURKA, AURKB, B2M, BAP1, BCL10.

BCL11B, BCL2, BCL2L2, BCL6, BCL7 A, BCOR, BCORL1, BCR, BIRC3, BRAF, BRCA1, BRCA2, BTG1, BTK, CALR, CARD11, CBFB, CBL, CCND1, CCND2, CCND3, CCNE1, CCR4, CCT6B, CD22, CD274, CD28, C

D58, CD79A, CD79B, CDK12, CDK4, CDK6, CDK8, CDKN1B, CDKN1C, CDKN2A, CDKN2B, CDKN2C, CEBPA, CHD4, CHEK1, CHEK2, CHUK, CITA, CKS1B, CRBN, CREBBP, CRLF2, CSF1R, CSF3R, CTLA4, CUL4B, CXCR4, DDB1, DDX3X, DDX41, DIS3, DKK1, DNMT 1, DNMT3A, DUSP2, DUSP9, EED, EGFR, EGR1, EP300, EPOR, ERG, ET NK1, ET S1, ETV1, ETV5, ETV6, EZH2, FAM46C, FAS, FBXW7, FGFR1, FGFR3, FLT3, FOXO1, FOXO3, FOXP1, FYN, GAT A1, GATA2, GATA3, GNA13, GNAI2, HDAC1, HDAC4, HDAC7, HIST 1H1C, HIST 1H1D, HIST 1H1E, HIST 1H2AC, HIST 1H2AG, HIST 1H2AL, HIST 1H2AM, HIST 1H2BC, HIST 1H2BJ, HIST 1H2BK, HIST 1H2BO, HIST 1H3B, HRAS, ID3, IDH1, IDH2, IKBKB, IKBKE, IKBKG, IKZF1, IKZF2, IKZF3, IL2RB, IL7R, IRAK1, IRAK4, IRF1, IRF4, IRF8, ITK, JAK1, JAK2, JAK3, JUN, KDM6A, KIT, KLHL6, KMT2A, KMT2B, KMT2C, KMT2D, KRAS, LEF1, LILRB1, LTB, LUC7 L2, LYN, MAF, MAG, MALT 1, MAP2K1, MAP2K2, MAP2K4, MAP3K1, MAP3K14, MAP3K6, MAP3K7, MAPK1, MCL1, MDM2, MDM4, MED12, MEF2B, MEF2C, MET, MPL,

MTOR, MUC2, MYC, MYCL, MYCN, MYD88, NCKAP5, NF1, NF2, NFATC2, NFKBIA, NOT CH1, NOT CH2, NPM1, NR3C1, NRAS, NT5C2, NTRK2, NTRK3, P2RY8, PAX5, PCLO, PDCD1, PDCD11, PDCD1LG2, PDGFRA, PDGFRB, PHF6, PIK3CA, PIK3CD, PIK3CG, PIK3R1, PIK3R2, PIM1, PLCG1, PPP3CA, PPP3B, PPP3CC, PRKCB, PRPF40B, PT EN, PT K2, PTK2B, PT PN11, RAD21, RARA, RASSF5, RB1, RHOA, RUNX1, SETBP1, SET D2, SF1, SF3A1, SF3B1, SH2B3, SMC1A, SMC3, SMO, SOCS1, SPP1, SRSF2, STAG2, STAT3, STAT5B, SYK, TAL1, TBL1XR1, TCF3, TET2, TNFAIP3, TP53, TSLP, TYK2, U2AF1, U2AF2, VAV1, WHSC1, WT1, XP01, ZFHX4, ZRSR2

DNA Gene List: For the Detection of Select Rearrangements

ALK, BCL6, TP63, DUSP22, MYC, BIRC3, BCL2

Table S3. FISH studies according to the presence of SSP

Variable	SSP	Non-SSP	*p*-value
MYC translocation (*N*=114)	(*N*=30)	(*N*=84)	
Present	7 (23.3%)	19 (22.6%)	*1.000*
Absent	23 (76.7%)	65 (77.4%)	
MYC copy number gain			
Present	3 (10%)	11 (13.1%)	*.758*
Absent	27 (90%)	73 (86.9%)	
BCL2 translocation (*N*=71)	(*N*=18)	(*N*=53)	
Positive	4 (22.2%)	7 (13.2%)	*.452*
Negative	14 (77.8%)	46 (86.6%)	
BCL2 copy number gain			
Positive	5 (27.8%)	5 (9.4%)	*.109*
BCL6 translocation (*N*=67)	(*N*=17)	(*N*=50)	
Positive	3 (17.6%)	16 (32.0%)	.356
Negative	14 (82.4%)	34 (68.0%)	
BCL6 copy number gain			
Positive	2 (11.8%)	3 (6.0%)	*.595*
Negative	15 (88.2%)	47 (94.0%)	

Supplementary Figure 1. Correlation between SSP and c-MYC expression

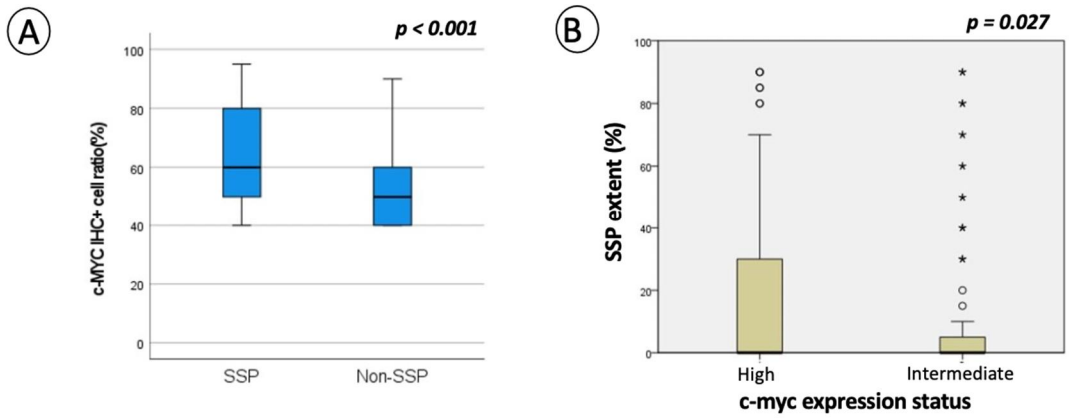

Supplementary Figure 2. Survival analyses according to morphologic subtype and the presence of tumor necrosis

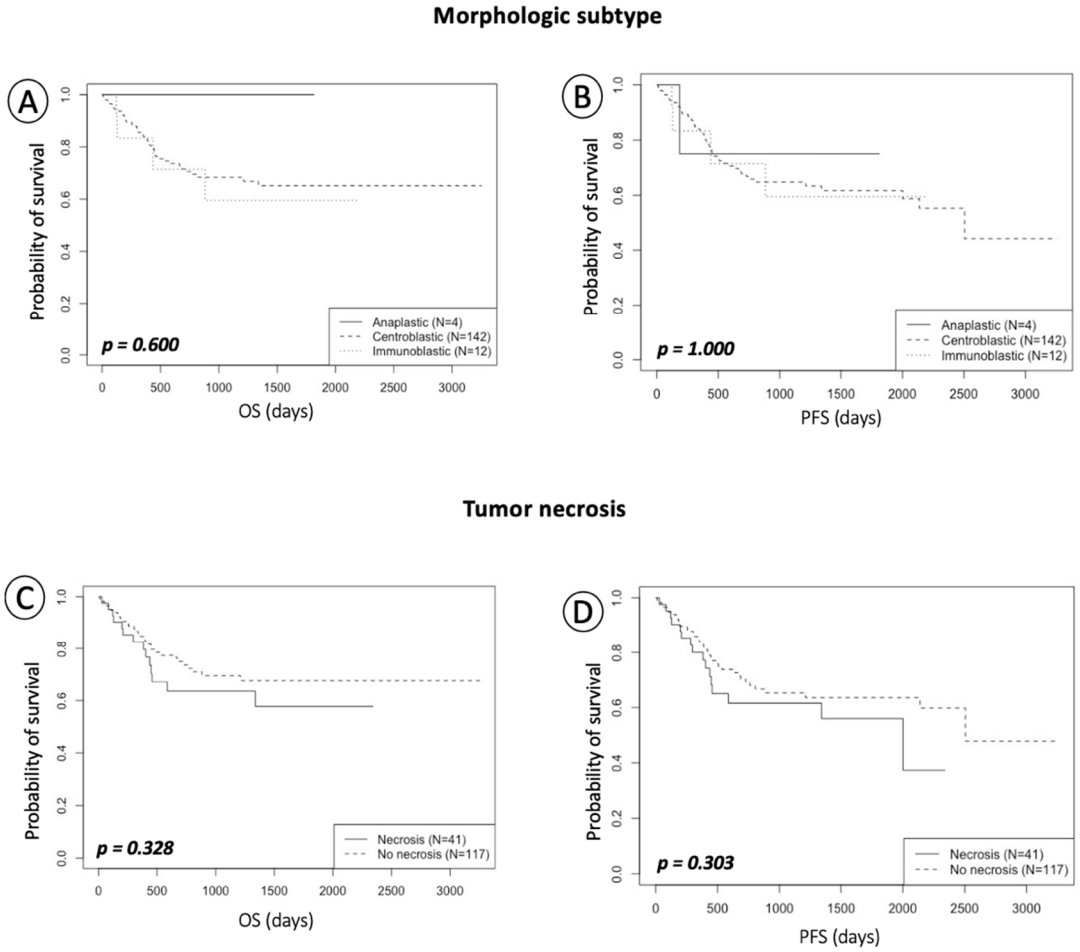

Supplementary Figure 3. Survival analyses in ABC subgroup according to SSP

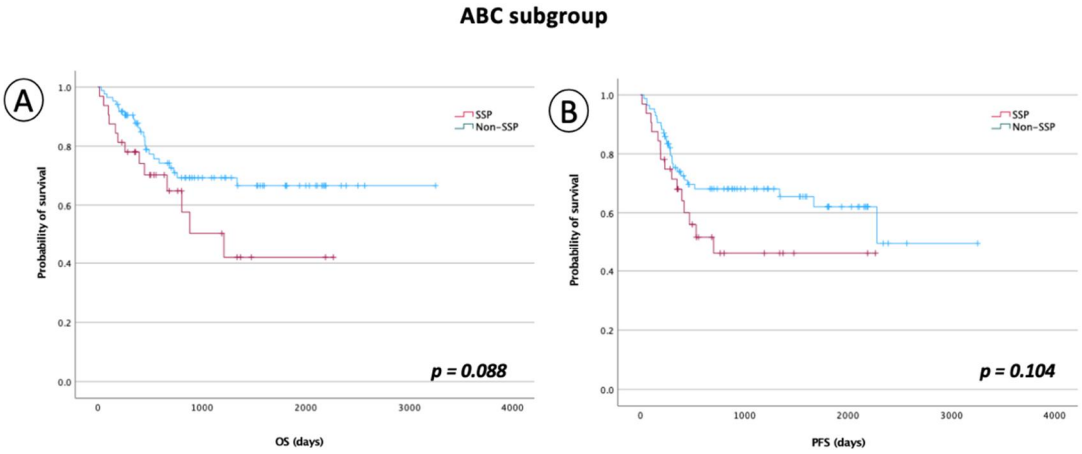

국문요약

이중 발현 림프종(DEL)은 예후가 좋지 않은 MYC 및 BCL2 단백질의 동시 발현을 특징으로 하는 미만성 거대 B 세포 림프종(DLBCL)의 하위 아형입니다. 그러나 DEL 의 형태학적 특징을 평가하기 위한 표준화된 기준은 현재까지 확립되지 않았습니다. 이번 연구에서 우리는 158 명의 DEL 사례에서 스테리-스카이 패턴(SSP)이 가지는 예후적 가치와 임상병리학적 및 유전적 특징과의 상관관계를 분석하는 것을 목표로 연구를 진행했습니다. SSP 는 c-MYC 과발현, CD5 발현, 높은 IPI 및 age-adjusted IPI 를 포함한 공격적인 매개변수와 유의하게 연관되었습니다. 단변량 생존 분석에서 SSP 의 존재는 낮은 무진행 생존기간(PFS)($p = 0.030$)과 관련이 있었고 불리한 전체 생존기간(OS) 경향이 있었습니다($p = 0.065$). 그러나 c-MYC 가 높게 발현되었을 때 SSP 는 열등한 전체 생존기간(OS)와 유의한 상관관계를 보였습니다 ($p=0.025$). 다변량 생존 분석에서 SSP 는 불량한 무진행 생존기간(PFS) 과도 관련이 있었습니다($p = 0.049$). 또한, 차세대 염기서열 분석에서는 SSP 그룹이 KMT2D 돌연변이와 유의미하게 연관되어 있으며 비 SSP 그룹과 다른 유전적 돌연변이 프로필을 가지고 있음을 보여주었습니다. 결론적으로 SSP 는 DEL 에서 공격성의 형태학적 특징을 나타낼 수 있음을 시사합니다.